Journal of Biomolecular NMR (2005) 31: 149–154

Spin-state selection for increased confidence in cross-correlation rates measurements

Paul R. Vasos, Jennifer B. Hall & David Fushman*
Department of Chemistry and Biochemistry, Center for Biomolecular Structure and Organization, University of Maryland, 1115 Agriculture/Life Sciences, Surge Bldg.(#296), College Park, MD 20742-3360, U.S.A.

Received 18 August 2004; Accepted 19 November 2004

Key words: chemical shift anisotropy, cross-correlation, relaxation interference, spin state selection

Abstract

A new approach is described for measuring chemical shift anisotropy (CSA)/dipolar cross-correlated relaxation (CCR) rates based on the selection of the individual ^{15}N doublet components prior to the relaxation period. The method uses the spin-state-selective element (S^3E) of Sørensen and co-authors [Meissner et al. (1997) *J. Mag. Reson.*, **128**, 92–97]. The main advantage of the new method compared to other *J*-resolved experiments is that it does not create problems of additional signal overlap encountered in coupled spectra. At the same time, this approach allows a simpler control of magnetization pathways than the indirect methods. The method is demonstrated for the B3 domain of protein G.

The quantitation of relaxation interference effects between chemical shift anisotropy (CSA) and dipolar interactions (Goldman, 1984) can provide valuable information about dynamics and local structure of molecules (e.g., Yang et al., 1997; Brutscher, 2000; Fushman and Cowburn, 2001; Schwalbe et al., 2001). In particular, measurements of ^{15}N CSA/dipolar cross-correlation rates can be used to characterize the overall and internal motions in proteins and nucleic acids (Tjandra et al., 1996b; Fushman et al., 1998; Kroenke et al., 1998; Boisbouvier et al., 1999; Dayie et al., 2002; Hall and Fushman, 2003a) and to determine the magnitude and orientation of ^{15}N chemical shift tensors in proteins (Fushman and Cowburn, 1998; Fushman et al., 1998); the latter information can be used for structure refinement (Lipsitz and Tjandra, 2003). The existing approaches to measuring rates of CSA/dipolar cross-correlated relaxation (CCR) can be divided in two classes (Carlomagno and Griesinger, 2000): *J*-resolved (or 'direct') and quantitative (or 'indirect') experiments.

The direct methods determine the CCR rate (η) from differential decay of the ^{15}N doublet components simultaneously observed in a ^{1}H-coupled spectrum (Hall et al., 2003; Hall and Fushman, 2003b). These experiments afford simple magnetization trajectories, at a cost of increasing signal overlap in the indirect dimension, where the resolution is limited and the signals can be severely crowded in large proteins. The overlap issue can be addressed by applying the IPAP scheme (Ottiger et al., 1998; Hall et al., 2003; Hall and Fushman, 2003b). However, this requires the addition and subtraction of two spectra obtained in the in-phase (IP) and anti-phase (AP) experiments, of which the second has an additional magnetization transfer element. The additional relaxation experienced in the AP experiment has to be compensated by a correction factor prior to the linear combination of the signals (Hall et al., 2003). While robust for non-overlapping peaks (Hall et al., 2003), the IPAP method could potentially introduce small variations in signal intensities when restoring overlapping peaks (see below).

The indirect approaches measure the rate of conversion of a selected coherence (N_y or $2N_yH_z$) into

*To whom correspondence should be addressed. E-mail: fushman@umd.edu

the complementary one due to the CCR effect. This is usually achieved via two separate experiments, A and B (e.g., Tjandra et al., 1996b; Tessari et al., 1997), wherein experiment A measures the build-up component (e.g. $2N_yH_z \rightarrow N_y$), while B serves as a reference experiment that detects the decay of the starting coherence ($2N_yH_z \rightarrow 2N_yH_z$). The published pulse sequences differ between experiments A and B in the number of pulses (Tjandra et al., 1996b) or in the order in which the selection elements are applied (Tessari et al., 1997). Imperfections in the parameters of these pulse sequences can lead to incomplete suppression of cross-correlated relaxation before and after the mixing period (Carlomagno and Griesinger, 2000) and can introduce deviations in the signal ratio between the two experiments that are difficult to quantify, as there is no direct control of the magnetization pathways. As shown in Pelupessy et al. (2003), four different experiments are required to completely balance differences in the evolution of the generated and detected operators in various pulse sequences using the indirect approach.

Here we propose a new direct method for measuring the cross-correlation rates that selects coherences (single-transition operators) corresponding to a given component of the ^{15}N doublet. The relaxation matrix pertinent to an isolated NH spin system is diagonal in the basis formed by the operators $\sigma_{up} = N_yH_z + N_y/2$ and $\sigma_{dn} = N_yH_z - N_y/2$, corresponding to the upfield and downfield components of the ^1H-coupled ^{15}N signal, provided the difference between the transverse relaxation rates of the in-phase and antiphase magnetization is negligible (this requirement can be circumvented by choosing relaxation delays as multiples of $1/J$, which would result in an averaging of the relaxation rate, R_2 (Ghose and Prestegard, 1998)). In order to adapt the experiment to the nature of the observable of interest, the corresponding coherences can be selected at the beginning of the CCR-relevant period. Their separate auto-relaxation rates, $R_2 \pm \eta$, can thus be determined directly, and there is no need to transfer to a pre-determined coherence (e.g., $2N_yH_z$) after the relaxation delay. Furthermore, the observed spectra are 'simplified' (compared to a ^1H-coupled HSQC) as the number of signals is the same as in the decoupled spectrum.

In order to generate the single-transition ^{15}N-operators we have used the spin-state-selective element (S^3E) of Sørensen and co-authors (Meissner et al., 1997). In the present implementation (Figure. 1), the S^3E selects either the σ_{up} or the σ_{dn} component at the beginning of the CCR delay 2Δ, depending on the phase cycle chosen. Alternative building blocks that perform the desired selection exist in the literature. Some of them aim at matching the duration of the intervals in which the IP and AP coherences are selected, one coherence being preserved as a double-quantum while the other one is allowed to evolve. This idea has been implemented in spin-state selective sequences such as the S^3ECT (Sørensen et al., 1997) and α/β-HSQC (Andersson et al., 1998); relaxation artifacts are known to occur with these approaches, as with the classical TROSY (Pervushin et al., 1997) at the position of the suppressed component, due to the difference between the relaxation rates of the double-quantum and single-quantum coherences (Rance et al., 1999). Other sequences select the σ_{up} or σ_{dn} transitions as linear combinations of the N_y and $2N_yH_z$ coherences in the same time interval as S^3E (Bouguet-Bonnet et al., 2003). We have chosen the S^3E building block because it can yield data with similar sensitivity to that of the IPAP sequence (Supplementary material), provided the scans for each of the selection phase cycles are stored separately and subsequently processed in linear combinations. The evolution of magnetization in terms of product operators during the selection element is detailed in Supplementary Table 1.

The application of the *S^3E filter-CCR period-^{15}N evolution without decoupling* formula presents the advantage that clean selection of the desired component can be directly monitored and controlled by adjusting the critical parameters of the sequence: the S^3E delay 2δ and the ^{15}N pulses (especially the 180° pulse in the middle of the selection filter). We verified this by comparing our experimental data with computer simulations using the Virtual NMR Spectrometer program (VSNMR) (Nicholas et al., 2000) (Figure 2). It can be shown using product operator analysis (Supplementary material) that a delay 2δ in the selection filter different from $2\delta_{opt} = 1/(4J)$ leads to a decrease of the selected component by a factor of $\cos[2\pi J(\delta - \delta_{opt})]$ and introduces an artifact signal in the spectra at the position of the unwanted component, with the intensity proportional to $-\sin[2\pi J(\delta - \delta_{opt})]$. The sign of the artifact is the same for both selected components and varies from positive to negative as a function of $\delta - 1/(8J)$.

Another critical factor for proper coherence selection is pulse calibration, particularly that of

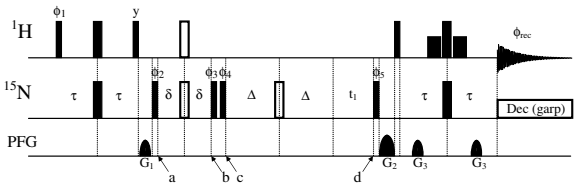

Figure 1. S^3E-selective pulse sequence for measuring transverse ^{15}N CSA-(^{15}N-^1H_N) dipole–dipole cross-correlation rates. Narrow and wide solid bars represent hard pulses with 90° and 180° flip angles, respectively. Open bars represent composite $90°_y$–$180°_x$–$90°_y$ pulses. Water suppression was achieved using two selective 1 ms-long low-power 90° ^{1}H pulses inserted in the reverse-INEPT step. The delays are: $\tau = 2.6$ ms; $\delta = 1.22$ ms; the duration of the CCR-relevant delay 2Δ is set to either zero or multiples of $1/J$. The relative intensities of the gradients are G1:G2:G3 = 1:2.3:1.4. Two experiments are run with different phase cycles selecting the $N_xH^\beta - N_yH^\alpha$ or $N_xH^\beta + N_yH^\alpha$ combinations, respectively. The phase cycling for the first experiment is φ_1 = x,−x, φ_2 = 4(45°), 4(225°); φ_3 = 2(x), 2(y); φ_4 = 2(x), 2(y); φ_5 = 8(x),8(−x); φ_{rec} = x, 2(−x), x, −x, 2(x), 2(−x), 2(x), −x, x, 2(−x), x while for the second experiment φ_2 = 2(2(45°), 2(225°)) and φ_4 = 2(−x),2(−y). The two resulting data sets are then added and subtracted to yield spectra containing the downfield and upfield components, respectively. Alternatively, this addition/subtraction can be performed by the spectrometer, when using the following phase cycle settings: φ_2 = 4(45°), 4(225°), 2(2(45°), 2(225°)); φ_3 = 2(x), 2(y); φ_4 = 2(2(x), 2(y)), 2(2(−x), 2(−y)); φ_5 = 16(x), 16(−x); and the receiver phase φ_{rec} = 2(x,2(−x),x,−x,2(x),−x),2(−x,2(x),−x,x,2(−x),x) for selecting the N_xH^β component and φ_{rec} = x,2(−x),x,−x,2(x),2(−x),2(x),−x,x,2(−x),x, −x,2(x),−x,x,2(−x),2(x),2(−x),x,−x,2(x),−x for the N_yH^α component. A constant-time version of the pulse sequence proposed here can be obtained in a standard way, by replacing the segment between the time points c and d with $(\Delta - t_1/2) - (180°_x\ ^{15}N) - (\Delta + t_1/2)$, thus including the t_1-evolution into the CCR period (as e.g. in (Hall et al., 2003)). It has the advantage that the signals in the indirect (^{15}N) dimension are not broadened by R_2 relaxation or CCR, hence its potential applications to systems where CCR delays longer than the maximum t_1-evolution delay can be explored. The data presented in this paper are for the 'real-time' version of the pulse sequence shown here; the ct-sequence yields similar results (Supporting Materials).

^{15}N pulses. This implementation uses composite 180° pulses ($90°_y$–$180°_x$–$90°_y$) in the selection module. A miscalibrated $180°_x$ ^{15}N pulse in the middle of the composite pulse results in a decrease in the intensity of the selected component by a factor $\cos(\alpha)$, where α is the deviation of the corresponding flip angle from 180°. In addition, spectral artifacts appear at the position of the unwanted component, with intensities proportional to $\sin(\alpha)$ if the upfield component is selected and $-\sin(\alpha)$ in the case of the downfield component. Consequently, artifacts caused by the imperfection of the 180° pulse in the middle of the composite pulse can be identified because they change sign depending on whether the pulse is longer or shorter than its ideal value. The experiment and VSNMR simulations show that similar effects, with additional phase distortions in the indirect dimension, occur when all ^{15}N pulses are miscalibrated (Figure 2c, d).

It should be noted that within the approximation that the relaxation matrix is diagonal in the representation of single-transition operators, the presence of an unwanted signal belonging to the complementary component should not directly affect the measurements, because the two components are resolved; errors are only introduced when this additional signal overlaps with that of another amide. The structure of the experiment proposed here is not only simpler than that of pulse schemes used in indirect methods, but it offers a way to monitor the correct settings of pulses and delays. For example, if a miscalibration of ^{15}N pulses is detected, the standard methods of pulse calibration can be used to correct it.

Some practical aspects of applying this method to proteins are worth mentioning here. The natural spread of the amide J-couplings observed in proteins (Tjandra et al., 1996a) is from 91 to 96 Hz or within ±2.7% from the mean. Assuming δ_{opt} is set using the mean value of J, this is expected to introduce artifacts up to 2% of the original intensity of this component. As mentioned above, this should not directly affect the ratio of the desired components. The effect of pulse imperfection due to off-resonance conditions is expected to be small over a ±15 ppm range typical for proteins when using hard 180° ^{15}N pulses (of about 70 μs pulse length). Indeed, the simulation shows that shifting the ^{15}N carrier by ±15 ppm introduced no noticeable change in the ratio of the up-field and downfield components. The intensity of the unwanted component observed in this case was similar to that for a 2% miscalibration of the ^{15}N pulse. Note also that, as a consequence of the sign difference (Figures 2c, d) between unwanted components introduced by shorter and longer ^{15}N pulses than the nominal value, the artifacts due to rf-inhomogeneity are expected to largely cancel out. Finally, our simulations and experiments suggest that miscalibrations of proton pulses primarily affect the sensitivity of the experiment.

The proposed method has been tested on the third IGG-binding domain of protein G (GB3) (Hall and Fushman, 2003a) at 500 and 600 MHz. The results obtained with the new method are in good agreement with those obtained using J-resolved-type pulse sequences (Hall et al., 2003; Hall and Fushman, 2003b) (Figure 3). For non-overlapping peaks, the values obtained with the new (S^3E-CCR)

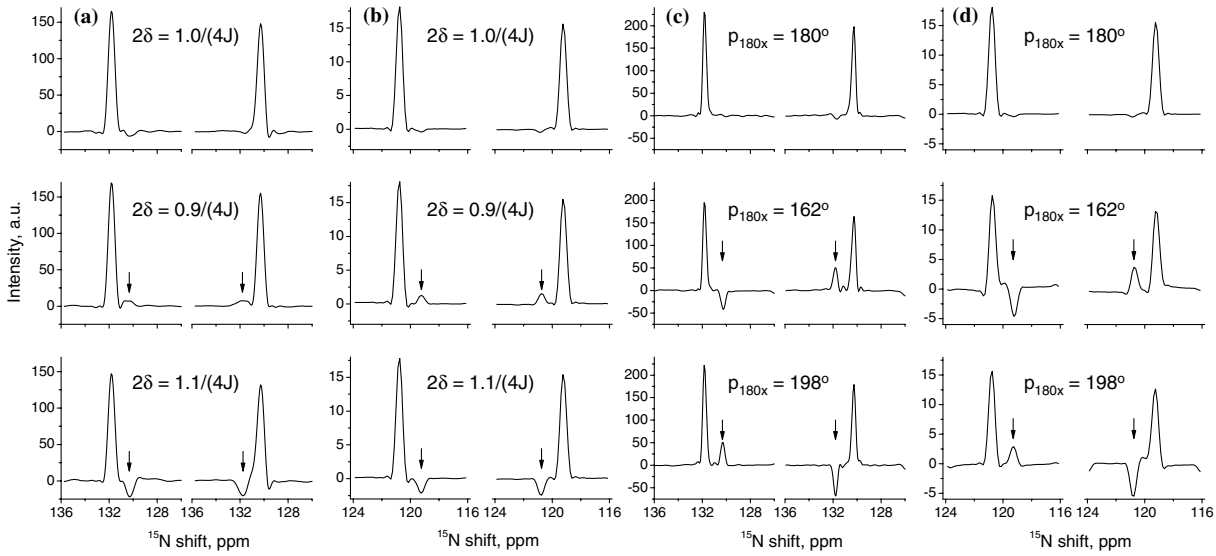

Figure 2. Cross-sections in the ^{15}N dimension of (a) experimental (at ^{1}H frequency 10.3 ppm, residue F52) and (b) simulated 2D spectra, for selection delays 2δ (Figure 1) set to an optimal value of $2\delta_{opt} = 1/(4J)$ (top panels) or to 90% (middle) or 110% (bottom) of $2\delta_{opt}$. Cross-sections of the (c) experimental and (d) simulated 2D spectra for various settings of the correct and miscalibrated ^{15}N pulses: optimal value (top), 90% (middle), and 110% of the optimal value (bottom). The left and right columns in each panel correspond to the selection of downfield and upfield components, respectively, of the doublet signal. The position of the unwanted component is indicated by arrows. The protein samples for NMR studies contained 0.9 to 1.4 mM of uniformly ^{15}N enriched GB3 dissolved in 30 mM phosphate buffer (pH 5.8) containing 9% D_2O.

sequence are expected to agree with those from the IP-only and IPAP methods (Hall et al., 2003; Hall and Fushman, 2003b), as the latter method is not sensitive to the exact value of the correction factor for the AP spectra (Hall et al., 2003). As far as the signal overlap is concerned, two cases have to be distinguished: (1) signals that already overlap in the decoupled spectra (these residues were excluded from the analysis), and (2) signals that overlap only in the coupled spectra, e.g. the up-field component of signal S_1 overlaps with the down-field component of another signal, S_2. In the second case, adding and subtracting the IP and AP spectra in the IPAP method should, in principle, restore the individual components. It can be shown, however, that errors in restored-peak intensities can arise from the difference in relaxation properties of the corresponding spins, resulting in a difference between the overall AP-correction factor f_0 and the signal-specific correction factors (f_1 and f_2) for signals S_1 and S_2. The relative error in the ratio of peak intensities of the up- and down-field components of S_1 can be approximated as $\delta(S_{1up}/S_{1dn})_{IPAP} \approx \frac{1}{2}\chi\,(S_{1up}/S_{1dn})(f_2 - f_0)$, where χ is the degree of overlap (i.e. the error in S_{1up} due to the overlap is $\delta S_{1up} = \chi S_{2dn}$), and we assumed that $f_1, f_2, f_0 \sim 1$. Although non-zero, this error is much smaller ($f_2 - f_0 << 1$) than that in the IP-only spectrum when the overlap is present: $\delta(S_{1up}/S_{1dn})_{IP} = \chi S_{1up}/S_{1dn}$. Considering that the difference between the overall and the signal-specific correction factors in GB3 is at most $\pm 5\%$, the error introduced in the IPAP approach is considerably smaller than that introduced by the untreated overlap. Overall, it can be concluded that CCR measurements via *J*-resolved experiments introduce relative errors in the signal ratios of the order of the degree of overlap for in-phase coupled spectra analyzed alone, about or less than 2.5% of the degree of overlap in IPAP experiments, and independent of the overlap when the S^{3}E method is used. Because of the different relaxation rates of S_{2dn} and S_{1up}, their ratio will depend on the CCR delay 2Δ, which in turn could affect the measured values of η.

Seven residues in GB3 show overlap only in the coupled spectra: K4, V5, A23, K24, A31, D47, A48 at 600 MHz and Q2, K4, V5, A23, D47, A48, V54 at 500 MHz (highlighted in Figures 3a–c); the peaks were considered overlapping if their centers were separated by less than 0.6 ppm in ^{15}N and 0.06 ppm in the ^{1}H dimensions. Of these residues, A23 was most affected by the overlap: neither IP nor IPAP data (600 MHz) could be fitted well to an exponential decay, whereas the S^{3}E data were fitted nicely. The results for the rest of the above-mentioned over-

lapping residues follow the expected trend, with IPAP data in better agreement with the S^3E results than the IP-derived values.

Figure 3d shows the correlation between CCR rates measured at 600 and 500 MHz using the spin-state-selective approach, and the IPAP method, for comparison. The measured η values exhibit a linear field dependence in agreement with the theoretical prediction ($\eta \propto CSA \propto B_0$, e.g. (Tjandra et al., 1996b)) consistent with the notion that the main contribution to CCR from dynamics arises from the spectral density component $J(0)$, while the $J(\omega_N)$ term is smaller and varies slowly with the field because the overall tumbling time of GB3 is close to $1/\omega_N$ (Hall and Fushman, 2003a). The good correlation between the two datasets thus confirms the quality of these data.

The proposed method was also compared with the indirect approach of (Tjandra et al., 1996b), herein called A/B (Figure 4). It has been noticed before (Hall et al., 2003) that there is a small although consistent underestimation (by 3–7%) of the CCR values derived using the A/B method. The imperfections in experimental settings alone were originally believed to be at the origin of this discrepancy. A careful analysis of the A/B pulse sequence (Tjandra et al., 1996b) indicates that the CCR transfer is not suppressed in the scheme B during the delay 2δ between time-point c and the beginning of the t_1 evolution period. It is, however, suppressed in scheme A due to the refocusing 180° ^1H pulse in the middle of the 2δ delay. The observed ratio of the signals in these experiments is therefore

$$S_A^{obs}/S_B^{obs} = \frac{\sinh(2\Delta\eta)}{\cosh[(2\Delta + 2\delta)\eta]}, \qquad (1)$$

where 2Δ and $2(\Delta+\delta)$ represent the total durations of the CCR-active periods in schemes A and B, respectively. This equation differs from the expected ratio, $S_A/S_B = \tanh(2\Delta\eta)$, by a factor $F = \cosh(2\Delta\eta)/\cosh(2\Delta\eta + 2\delta\eta) \approx 1 - 2\delta\eta\cdot\tanh(2\Delta\eta)$. F decreases with the delay Δ and plateaus at $1 - 2\delta\eta$ for $\Delta > 1/\eta$. Fitting the experimental data to $S_A^{obs}/S_B^{obs} = \tanh(2\Delta\eta)$ instead of Equation 1 will result in the underestimation of the actual cross-correlation rate. Calculations show that in GB3 under our experimental conditions the error in η varies from 0.4 to 1.3%. This error is small but could increase for higher magnetic fields and/or bigger proteins (as η increases) and for longer CCR-evolution delays Δ. For example, for a protein of twice the molecular weight of GB3 ($\eta \sim 7.5\ s^{-1}$) $F = 0.98$ for the same value of $\Delta\cdot\eta$, and the expected error in η is 2.2%. The remaining 2–5% difference between the direct measurements (IP/IPAP or

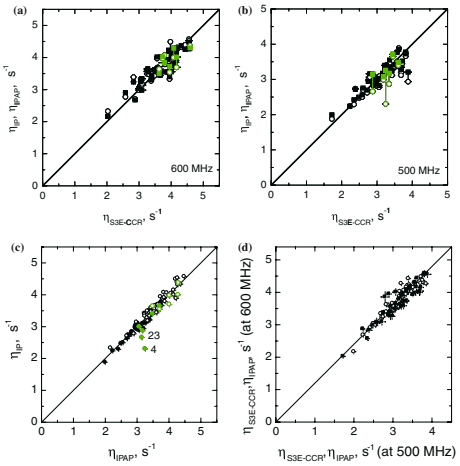

Figure 3. (a) The agreement between the cross-correlation values ($\eta_{S3E\text{-}CCR}$) obtained using the spin-state-selective sequence and IPAP (open circles) or IP (solid squares) methods [Hall, 2003 #10875] for GB3 at 600 MHz. The IP and IPAP-derived values for each residue are connected by vertical lines. The correlation coefficient is 0.90 (S^3E vs. IPAP) and 0.91 (S^3E vs. IP) (for non-overlapping residues). The error bars represent stochastic errors, calculated based on measured signal-to-noise ratio in the spectra. The data points for residues affected by signal overlap in the coupled spectra are colored green. The η values were derived by fitting the ratio of peak intensities to $C\cdot\exp(-4\eta\Delta)$, where C is a constant reflecting differences in signal intensities of the two components introduced by relaxation processes during the t_1 period (independent of Δ) in Figure 1 (Hall and Fushman, 2003b). The experiments were recorded with 2048 points in t_2 and 128 increments in the indirect dimension. Each pair of experiments was performed in an interleaved fashion. The number of transients, 16 or 32 depending on the delay Δ was the same for both experiments, with the recycling delay of 1.2 s, resulting in a total experiment time of 1 h 45 min or 3.5 h for a set of two experiments. The values of Δ were set to 0, 10.64, 21.28, 31.92, 42.55, and 53.19 ms for IPAP and 0 (x2), 10.64, 21.28, and 42.55 ms for S^3E. These measurements were performed on Bruker DRX-600 spectrometer equipped with a triple-resonance cryoprobe. (b) The same correlation as in panel A, for data measured at 500 MHz. The correlation coefficient was 0.91 (S^3E vs. IPAP) and 0.87 (S^3E vs. IP). These measurements were performed on Bruker DRX-500 spectrometer equipped with a conventional triple-resonance probe, using similar experimental settings as in panel (a) with the Δ-delays of 0 (x2), 10.64, 21.28 (x2), 42.55, and 53.19 ms, for both S^3E and IPAP (the duplicate points refer to S^3E measurements), and 32 or 64 transients. The outlier (K50) is a borderline case for our definition of overlapping residues in the coupled spectra. (c) The agreement between the η values measured using IP and IPAP methods at 600 MHz (open circles) and 500 MHz (solid circles). Data for the overlapping residues are colored green, K4 and A23 are most affected by the overlap in coupled spectra. (d) Correlation between the cross-correlation rates measured at 600 MHz and at 500 MHz. Data obtained using the spin-state-selective approach (solid squares) and the IPAP method (open circles) are shown for comparison. The slope of the line (= 1.2) represents the ratio of the field strengths. The correlation coefficients are 0.93 (S^3E) and 0.94 (IPAP).

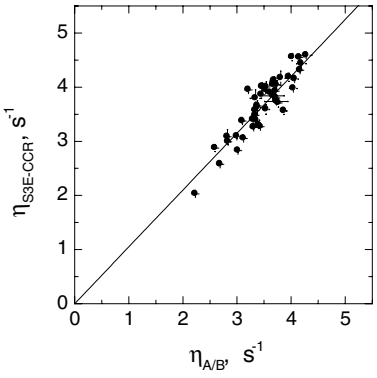

Figure 4. The agreement between the cross-correlation rate values (at 600 MHz) obtained using the proposed method and those derived previously (Hall et al., 2003) using the indirect method (A/B) of (Tjandra et al., 1996b). The correlation coefficient between these data is 0.91. The A/B measurements were performed twice, using a room-temperature probe (Δ delays set to 31.92, 42.55, 53.19, and 63.82 ms (Hall et al., 2003)) and a cryoprobe, with the Δ delays of 53.2 (x2) and 63.8 ms; the two sets of $\eta_{A/B}$ values are in good agreement with each other (correlation coefficient of 0.99). Shown here are the $\eta_{A/B}$ data from the cryoprobe measurements corrected for the unsuppressed CCR transfer during coherence selection in experiment B (see text for details). The slope of 1.05 of the line probably reflects unaccounted for imperfections in the experimental settings in the A/B experiment (see also Hall et al., 2003).

S3E-CCR) and the A/B method in GB3 (Figure 4) has to be accounted for by the imperfections in the experimental settings in the A/B measurements. In particular, a mismatching in the duration of δ or pulse imperfections will primarily result in incomplete in-phase to antiphase conversion in scheme A, which would further reduce the observed S_A/S_B ratio.

In conclusion, the experimental approach presented here provides a robust method for ^{15}N CSA/dipolar cross-correlation rate measurements, alleviating problems encountered in the existing methods such as magnetization transfer via unwanted pathways or additional resonance overlap. The advantage of the new sequence over the IPAP experiment is that it provides 'simplified' spectra and thus reduces errors due to signal overlap caused by doubling of peaks in coupled spectra. Its advantage over the indirect pulse sequences is in the spectral separation of the desired and unwanted signals, hence experimental missettings due to miscalibrated pulses and/or delays do not affect the measurements and can be directly identified. Any imperfections in the quantitative pulse sequences lead to magnetization leaks via relaxation which are expected to increase with the increase in the overall tumbling time. Furthermore, the occurrence of overlap in the indirect dimension in coupled spectra is expected to increase with protein size. The proposed approach is therefore particularly well suited for measurements on large molecules, where previously proposed methods may be prone to inaccuracy.

Acknowledgements

Supported by grants from NIH (GM65334) and NSF (DBI-0138000) to D.F.

Supplementary material to this paper is available in electronic form at http://dx.doi.org/10.1007/s10858-004-7562-8.

Note added in proof: After the submission of the present manuscript, CCR measurement has been published (Bouguet-Bonnet et al. *J. Biomol. NMR* **30**: 113–142, 2004) that utilizes a spin-state selective element of lesser sensitivity than S^3E. The use of ^{1}H decoupling during t_1-evolution in that paper prevents separation of the desired and unwanted signals, making that approach susceptible to experimental settings.

References

Andersson, P. et al. (1998) *J. Magn. Reson.,* **133**, 364–367.
Boisbouvier, J. et al. (1999) *J. Biomol. NMR,* **14**, 241–252.
Bouguet-Bonnet, S. et al. (2003) *Magn. Reson. Chem.* **41**, 1030–1033.
Brutscher, B. (2000) *Concepts Magn. Reson.,* **12**, 207–229.
Carlomagno, T. and Griesinger, C. (2000) *J. Magn. Reson.,* **144**, 280–287.
Dayie, K.T. et al. (2002) *J. Mol. Biol.,* **317**, 263–278.
Fushman, D. and Cowburn, D. (1998) *J. Am. Chem. Soc.,* **120**, 7109–7110.
Fushman, D. and Cowburn, D. (2001) In *Methods in Enzymology*, Vol. 339, James, T., Schmitz, U. and Doetsch, V. (Eds.), pp. 109–126.
Fushman, D. et al. (1998) *J. Am. Chem. Soc.,* **120**, 10947–10152.
Ghose, R. and Prestegard, J.H. (1998) *J. Magn. Reson.,* **134**, 308–314.
Goldman, M. (1984) *J. Magn. Reson.,* **60**, 437–452.
Hall, J.B. and Fushman, D. (2003a) *J. Biomol. NMR,* **27**, 261–275.
Hall, J.B. and Fushman, D. (2003b) *Magn. Reson. Chem.,* **41**, 837–842.
Hall, J.B. et al. (2003) *J. Biomol. NMR,* **26**, 181–186.
Kroenke, C.D. et al. (1998) *J. Am. Chem. Soc.,* **120**, 7905–7915.
Lipsitz, R.S. and Tjandra, N. (2003) *J. Magn. Reson.,* **164**, 171–176.
Meissner, A. et al. (1997) *J. Magn. Reson.,* **128**, 92–97.
Nicholas, P. et al. (2000) *J. Magn. Reson.,* **145**, 262–275.
Ottiger, M. et al. (1998) *J. Magn. Reson.,* **131**, 373–378.
Pelupessy, P. et al. (2003) *J. Magn. Reson.,* **161**, 258–264.
Pervushin, K. et al. (1997) *Proc. Natl. Acad. Sci. USA,* **94**, 12366–12371.
Rance, M. et al. (1999) *J. Magn. Reson.,* **136**, 92–101.
Schwalbe, H. et al. (2001) *Meth. Enzymol.,* **338**, 35–81.
Sørensen, M.D. et al. (1997) *J. Biomol. NMR,* **10**, 181–186.
Tessari, M. et al. (1997) *J. Magn. Reson.,* **127**, 128–123.
Tjandra, N. et al. (1996a) *J. Am. Chem. Soc.,* **118**, 6264–6272.
Tjandra, N. et al. (1996b) *J. Am. Chem. Soc.,* **118**, 6986–6991.
Yang, D. et al. (1997) *J. Am. Chem. Soc.,* **119**, 11938–11940.